Chemical Engineering Journal 155 (2009) 925–930

Contents lists available at ScienceDirect

Chemical Engineering Journal

journal homepage: www.elsevier.com/locate/cej

Surfactant assisted hydrothermal and thermal decomposition synthesis of alumina microfibers with mesoporous structure☆

Zhenfeng Zhu*, Hui Liu, Hongjun Sun, Dong Yang

School of Materials Science and Engineering, Shaanxi University of Science and Technology, Xi'an 710021, PR China

ARTICLE INFO

Article history:
Received 22 June 2009
Received in revised form
15 September 2009
Accepted 19 September 2009

Keywords:
Mesoporous alumina
Microfibers
Hydrothermal synthesis
SCR-NH_3 of NO

ABSTRACT

The alumina microfibers with mesoporous structure were synthesized by a facile hydrothermal and thermal decomposition route. The as-obtained products were well characterized by XRD, SEM, TEM (HRTEM), SAED and N_2 adsorption–desorption measurement. It was shown that the length and diameter of these alumina microfibers are about 10 μm and 300–500 nm, respectively. All these alumina microfibers prepared by the PEG templates with different molecular weight have the different high surface area but nearly the same pore diameter about 3.5 nm. The calcination experimental result shows that the mesoporosity of these alumina microfibers can be maintained even at 1373 K. On the other hand, the higher selective catalytic reduction (SCR) of NO effectiveness present that the as-obtained mesoporous alumina have stronger adsorption property because of its high surface area.

1. Introduction

Mesoporous materials have been intensively studied with regard to technical applications as catalysts and catalyst supports [1–3]. In which, mesoporous alumina has been extensively used as advanced catalysts and catalyst supports due to its low cost, good thermal stability and high specific surface area [4–6]. For specific applications, the mesoporous properties, such as the surface area, the pore size and pore volume of the support, have a large impact on the catalytic effect. Therefore, great efforts are made to produce porous alumina with tailored properties to suit different applications using anionic, cationic or non-ionic surfactants as structure directing agents [7–10]. In these methods, the surfactant can assembly with the inorganic species to form mesostructured pore structures and then different surfactants may induce different microstructures. All of these efforts obtained the mesoporous alumina with adjusting surface area, pore size and pore volume by using different surfactants. Different from the mechanism of cooperative assembly from the starting molecular species commonly under the presence of mesoporous structure directing templates, the recent literatures report a new strategy to synthesis mesoporous materials by a controlled thermal decomposition process, in which the mesopores are generated via the thermal decomposition of the salts precursors [11,12]. In such an approach, gases (such as CO_2, CO, water and so on) are generated with the remarkable shrinkage in the framework of the materials during the thermal decomposition process, and finally oxides are obtained if the process is in air/O_2 atmosphere. Therefore, it is possible to create porous materials easily by controlling the thermal decomposition process, i.e., preventing extensive shrinkage during the decomposition of salts, which is most important to remaine the morphology of the nanostructural mesoporous materials. As the best of our knowledge, no report has been available on the synthesis of mesoporous alumina with adjusting mesoporous properties by using this thermal decomposition approach. On the other hand, the porous alumina have usually been functionalized and tested in laboratory scale for use as adsorbents or as catalysts for different chemical reactions [13,14]. However, alumina can have relatively low thermal stability over time. This is especially true for the porous materials and limits to their usefulness at high temperature. Fortunately, using the advantage of preventing extensitive materials shrinkage during the decomposition of salt precursors, the obtained mesoporous alumina may have relatively high thermal stability.

Herein, we describe a facile hydrothermal route to synthesize uniform ammonium aluminum carbonate hydroxide (denoted as AACH) microfibers with a high yield in the presence of non-ionic surfactant poly ethylene glycols (PEG) with different molecular weight, which has been shown to be a templating agent to the formation of 1D nanostructure materials [15–18]. The morphology-remained mesoporous alumina microfibers with adjusting surface area and pore volume but nearly the same pore size were readily obtained by thermal decomposition of the as-obtained AACH

☆ We acknowledge financially supported from the National Science Foundation of China (No. 50772064) and China Postdoctoral Science Foundation Founded Project (No. 20080440185).

* Corresponding author. Fax: +86 29 86168802.
E-mail address: zhuzf@sust.edu.cn (Z. Zhu).

1385-8947/$ – see front matter © 2009 Elsevier B.V. All rights reserved.
doi:10.1016/j.cej.2009.09.030

products. Finally, the adsorption property of these mesoporous materials as the catalyst support was measured by means of SCR technology.

2. Experimental

2.1. Preparation of mesoporous materials

Mesoporous materials were prepared through the hydrothermal reaction of a mixture composed of aluminum sources, surfactant, pH adjusting regent and solvents. All chemicals are analytical-grade regent without further purification. The surfactants used in this study were poly-glycol (PEG) (Kermel, 99%) with different molecular weight (M_n = 400, 1000, 2000, 4000 and 20,000, respectively), while the pH adjusting agent used was urea.

In a typical synthesis, an amount of surfactant PEG was dissolved in deionized water to form a clear solution, to which 2.0 mmol $Al(NO_3)_3{\cdot}9H_2O$ was added. After the aluminum salt was totally dissolved, 0.36 mol of urea was added. The mixed solution was further magnetically stirred for 3 h. Then the final mixture was transferred to a Teflon-lined stainless-steel autoclave and place in an oven at 413 K. After 24 h, the autoclave being cooled to room temperature, the white precipitation were collected and washed several times with deionized water and ethanol to remove the impurities and then dried at 353 K in a vacuum oven for 24 h. The surfactant was removed by calcination in air at 773 K for 2 h with heating rate of 1 K/min. To study the phase transformation and thermal stability, calcination was also conducted at 973, 1173, 1373, and 1573 K in a temperature-programmed Muffle furnace, respectively.

2.2. Characterization of mesoporous materials

The small- and wild-angle XRD patterns of the mesoporous materials were recorded on a high resolution X-ray diffractometer (XRD, D/MAX 2200pc, Japan). Their diffraction patterns were obtained by using Cu Kα radiation of wavelength λ = 0.15418 nm.

The morphology of the mesoporous alumina was recorded by using a field-emission scanning electron microscope (JSM-6700F, JEOL Japan) operated at 5 kV. The arrangement of the mesopores of the mesoporous materials was observed by means of a transmission electron microscope (JEM 2010 from JEOL, Japan) operated at 200 kV.

A volumetric adsorption measurement system (Quantachrome Nova2000e surface area and pore size analyzer) was employed to measure the adsorption/deposition isotherms of nitrogen on the mesoporous materials. The samples were evacuated at 773 K for 2 h before exposing them to nitrogen at 77 K. Their surface was calculated by the Brunauer–Emmett–Teller (BET) equation and their average pore diameter by the Barrett–Joyner–Halenda (BJH) method.

The adsorption property of the mesoporous materials as the catalyst support was measured by using a quartz fix-bed flow reactor heated with a furnace [19], and 3.0 g mesoporous materials with a diameter of 1 cm and a length of 5 cm were used. The feed gas mixture contained 1000 ppm NO, 1000 ppm NH_3, 500 ppm O_2 and nitrogen as balance gas, unless otherwise specified. The effluent gases from the reactor were analyzed on-line by a quadrupole mass spectrometer previously calibrated with cylinders of known concentrations. The NO conversion was calculated by means of the following reaction:

$$\%\ \text{NO reduction} = \frac{C^i_{NO} - C_{NO}}{C^i_{NO}} \times 100 \quad (1)$$

where C^i_{NO} is the initial concentration of NO and C_{NO} corresponds to its concentration once steady state is reached.

3. Results and discussion

Parts A and B of Fig. 1 show that the SEM micrographs of the precursor of hydrothermally prepared AACH prior to further heat treatment, it is seen that the sample is made of uniformly sized microfibers. These fibers were not tangled or interwound. The length of the fibers is about 10 μm. The magnified SEM image depicted in Fig. 1B (shown as inset) reveals that the fibers have a very smooth surface, and both the ends of the fibers shrinked to a needle-like structure. The inset of AACH precursor shown in Fig. 1B also reveals that the fiber has a columniform shape with a diameter of about 300–500 nm. Fig. 1C shows the typical XRD pattern of the as-synthesized sample (PEG-20000), and the XRD patterns of all as-synthesized samples in our experiments can be indexed to crystalline ammonium aluminum carbonate hydroxide (AACH) with a composition of $NH_4[Al(OOH)HCO_3]$ (JCPDS card no. 42-0250) [20–24], which is conventionally synthesized by reaction of aluminum sulfate with ammonium hydrogen carbonate in the liquid phase. Recently, Bai et al. reported the synthesis of AACH using the copolymer controlled homogeneous precipitation route [25]. In our experiment, using PEG with different molecular weight, we also obtained the AACH microfibers. The high intensities of the XRD peaks of the as-synthesized samples indicate that the AACH phase synthesized in this work is high crystalline. The highly intensity of the (1 1 0) crystal face also exhibits that the AACH crystal preferably grew along the given direction under the synthesis conditions. No other diffraction peaks were detected, indicating that no impurity exists in the AACH precursor. Using the Scherer equation, the calculated crystallite size of AACH microfibers is about 5.983 nm. The further experimental results exhibited that although the PEG with different molecular weight were used, the as-synthesized samples have the same morphology when the molar ratio of $Al(NO_3)_3$ to PEG is controlled to 0.02. If there are no further explanation, all samples shown in this manuscript is prepared with the Al/PEG molar ratio of 0.02. This result indicates that the surfactants PEG with different molecular weight have the same effect on the forming of the fiber-like as-synthesized samples. Fig. 1D shows the SEM images of alumina prepared in the absence of PEG. It is seen that the sample prepared in the absence of PEG exhibited an irregular particle morphology with some rodlike particles.

Fig. 2 presents the TEM images and SAED patterns of the AACH precursor (Fig. 2A and B) and the calcined samples synthesized using PEG-20000 at 773 K (Fig. 2C and D), 1173 K (Fig. 2E and F) and 1573 K (Fig. 2G and H) for 2 h, respectively. Fig. 2A shows the TEM image of the AACH microfibers. The SAED pattern (Fig. 2B) recorded from the face of the crystal having the longest axis (for example, the circled area in the TEM image) always exhibits the same single-crystalline pattern, consistent with the [0 0 1] zone of AACH crystals. The elongated microfiber shape with the exposed (0 0 1) faces demonstrated that the AACH crystal preferably grew along the crystallographic *c* axis under the synthesis conditions. Fig. 2C, E, and G shows the TEM images of the calcined samples at 773 K, 1173 K and 1573 K for 2 h, respectively. It can be seen that the diameter of the microfibers decreased after calcination process, this may be caused by the thermal decomposition of AACH in the calcination process. On the other hand, the morphology of the alumina microfibers was not markedly altered. With the increasing of the calcination temperature, the alumina fibers became some curved, however the essential fiber morphology still remained. It is also can been seen that, with the calcination temperature increase to 773 K or 1173 K, the surface of the fibers became more and more corrugated. As is know, the structure of AACH crystal is composed of Al–O octahedron chains linked by covalently sharing oxygen atoms. CO_3^{2-} and NH_4^+ ions are located between the chains associated by weak bonds, such as hydrogen bands. During the decomposition of AACH, the Al–O bonds remain unchanged while the weaker bonds

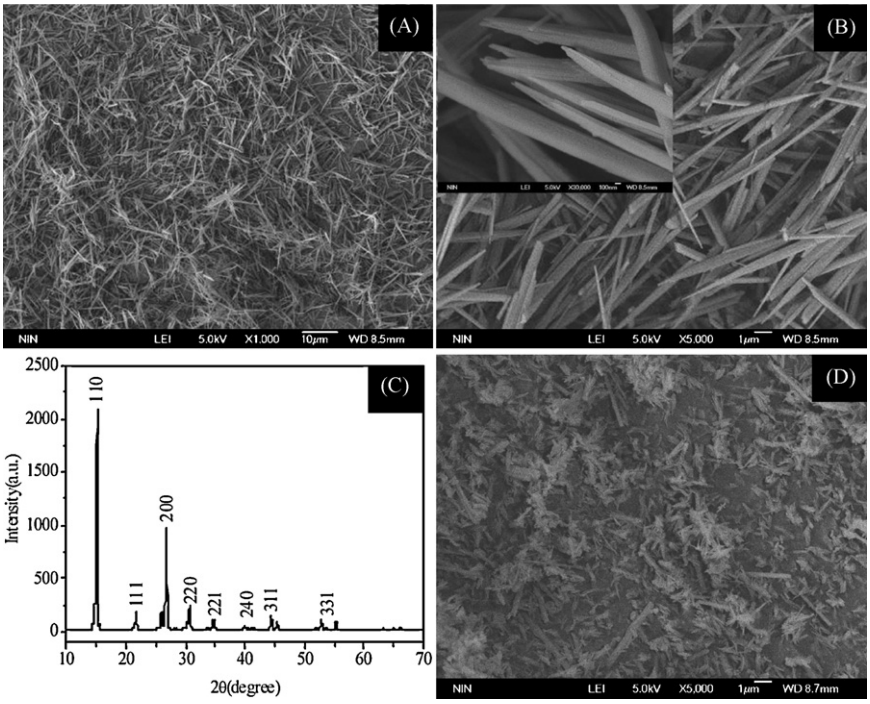

Fig. 1. SEM micrographs of as-synthesized AACH precursor (A and B), (C) XRD patterns of the AACH precursor, and (D) SEM micrographs of as-synthesized AACH precursor in the absence of PEG.

between CO_3^{2-} and NH_4^+ ions and Al–O octahedron chains are broken, releasing NH_3, CO_2 and H_2O [24,26,27]. This special structure of AACH endows the alumina microfibers with high thermal stability. During the thermal decomposition process, the AACH precursor does not cause dramatic change of the framework, therefore, the net-liked morphology and the size of the particles remain almost unchanged, but cracks may be formed and developed in the crystals as temperature increases. This is beneficial to the remaining of the fiber-like morphology and mesoporous structure. However, when the calcination temperature was increased to 1573 K, the surface of the fibers became smooth again (see Fig. 2G), possibly because of sintering. The selective area electron diffraction (SAED) patterns of the alumina fibers indicate that, with the increasing of the calcination temperature, the AACH precursor thermally decomposed and transformed to amorphous (Fig. 2D), polycrystalline (Fig. 2F) and single-crystalline alumina after calcination at 773 K, 1173 K and 1573 K, respectively.

In order to further identify the phase transform of the alumina microfibers during the calcination process, the XRD patterns of the calcined products of AACH precursor at different temperature are measured. Fig. 3 shows the XRD patterns of the sample prepared by using PEG-2000 calcined at different temperatures. After calcination at 773 and 973 K, both alumina samples essentially became amorphous. By increasing the calcination temperature to 1173 K, the γ- and θ-Al_2O_3 phases were observed. The low intensity of the XRD peaks indicates the alumina samples calcined at this temperature has a low crystalline, while the broad peaks demonstrated that the alumina fibers calcined at 1173 K are nanocrystalline, consistent with the previous results [26]. Further increasing the calcination temperature to 1373 K, the α-Al_2O_3 phase is observed. When the

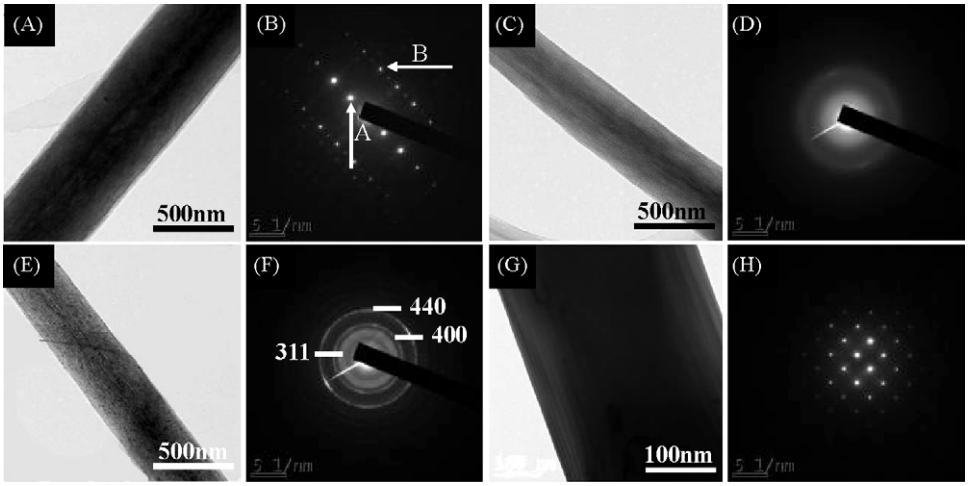

Fig. 2. TEM images and SAED patterns of the AACH precursor (A and B) and calcined samples at 773 K (C and D), 1173 K (E and F) and 1573 K (G and H) for 2 h synthesized using PEG-20000, respectively. The SAED pattern B is conformed to be [0 0 1] zone of the AACH crystal (reflections: A (0 2 0); B (2 0 0)) and indicates the direction of AACH microfiber growth is perpendicular to the [0 0 1] crystallographic axis.

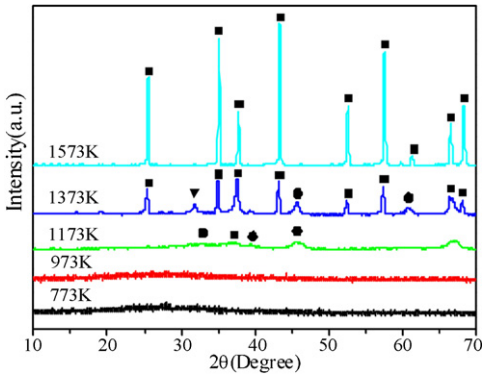

Fig. 3. Wild-angle XRD patterns of as-synthesized samples calcined at different temperatures for 2 h. (■), (●) and (▼) denote the α-Al_2O_3, γ-Al_2O_3 and θ-Al_2O_3, respectively.

calcination temperature increasing to 1573 K, a typical XRD pattern of the α-Al_2O_3 phase (JCPDS Card no. 46-1212) was obtained. The shape and high intensities of the peaks indicate that the Al_2O_3 phase is indeed well crystallized. All of the peaks can be index to α-Al_2O_3, and the measured lattice constants of *a* and *c* of this hexagonal phase are 4.763 and 12.987 Å, respectively, which is in good agreement with theoretical values ($a = b = 4.759$ Å and $c = 12.993$ Å, respectively). No other diffraction peaks were detected, indicating that no impurity exists and the precursor have completely transformed into the α-Al_2O_3 phase.

Fig. 4 shows that the TEM images of the typical alumina fiber obtained after calcination of the AACH precursor at 773 K (Fig. 4A–C) and 1373 K (Fig. 4D) for 2 h at different magnifications. After calcination at 773 K (Fig. 4A–C), it can been seen that the mesoporous alumina microfibers prepared by PEG templates with different molecular weight show wormhole-like appearance and no significant order in pore arrangement. This is in good agreement with absence of high order peaks in X-ray diffraction pattern (see curve 773 K in Fig. 3). In this paper, the surfactant PEG is not used as a directing template for the mesoporous structure but for the fiber-like structure, and the mesopores are generated via the thermal decomposition of salt precursor AACH from nanometer sized polyhedron particles, which is totally different from the mechanisms of cooperative assembly from the starting molecular species commonly under the presence of mesoporous structure directing templates. Thus, the obtained mesoporous alumina microfibers show no significant order in pore arrangement. After calcination at 1373 K (Fig. 4D), although the formation and afterwards crystallite growth of α-Al_2O_3 phase, together with the interparticle sintering and increasing of the grain size, result in the dramatically decrease of the wormhole-like mesopores, the surface of the fibers is still corrugated, showing the existence of the wormhole-like mesopores structure. The N_2 adsorption–desorption experimental result shown that the pore volume and surface area of the alumina microfibers prepared with PEG-400 retained at about 0.28 cc/g and 87 m^2/g, respectively. These indicate that the mesoporosity of this alumina material can be maintained at 1373 K and the prepared alumina microfibers using have the high thermal stability.

Fig. 5 shows the N_2 sorption isotherms and BJH pore size distribution curves of the samples prepared by PEG templates with different molecular weight, respectively. All isotherms are of typical type IV with hysteresis loop, indicating the alumina microfibers are mesoporous materials. All samples synthesized in the presence of PEG displayed steep capillary condensation and evaporation steps within the pressure range of $P/P_0 = 0.4$–0.7, implying they have a narrow mesopore size distribution. This is also confirmed by the BJH pore size distribution curves of the samples prepared by PEG templates with different molecular weight (Fig. 5B). All BJH pore size distribution curves show a narrow normal distribution between 2 and 5 nm, and the pore size distribution centered at about 3.5 nm pore diameter. The characteristics of the mesoporous alumina microfibers prepared by PEG templates with different molecular weight after calcination at 773 K for 2 h were shown in Table 1. It can been seen that, although prepared by PEG templates

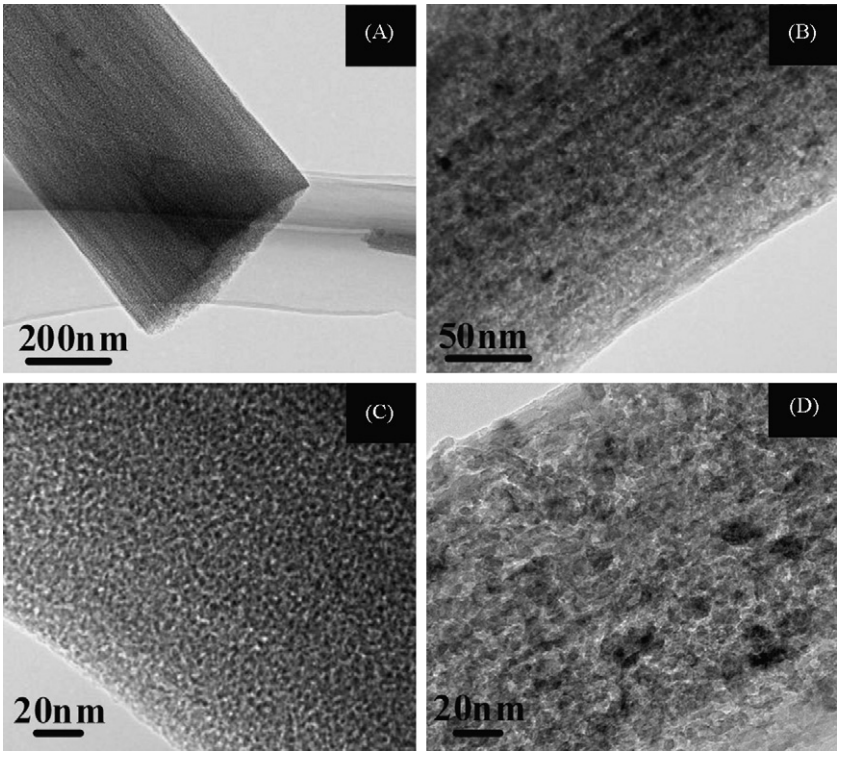

Fig. 4. TEM images of the typical alumina fibers after calcination at 773 K (A–C) and 1373 K (D) for 2 h at different magnifications.

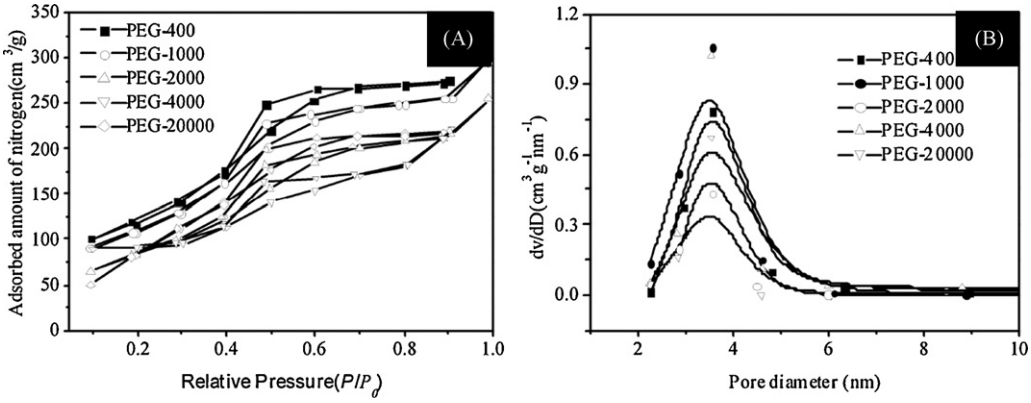

Fig. 5. Nitrogen adsorption–desorption isotherms (A) of mesoporous alumina microfibers prepared by PEG with different molecular weight and its pore size distribution (B). Calcination condition: 773 K, 2 h.

Table 1
Characteristics of the mesoporous alumina microfibers. Calcination condition: 773 K, 2 h.

Alumina microfibers	Molecular weight of PEG	BET surface area (m^2/g)	Total pore volume (cc/g)	BJH pore diameter (nm)
Al_2O_3-1	400	465	0.66	3.5641
Al_2O_3-2	1,000	406	0.57	3.5561
Al_2O_3-3	2,000	373	0.38	3.5670
Al_2O_3-4	4,000	282	0.35	3.5441
Al_2O_3-5	20,000	356	0.42	3.5446

The pore diameters were calculated from the desorption branches of their nitrogen adsorption–desorption isotherms.

with different molecular and all samples have the different BET surface area and total pore volume, the BJH pore diameter of all samples are same about 3.5 nm. The little changes in the BJH pore diameter of the mesoporous alumina microfibers prepared by PEG templates with different molecular weight may be caused by the tiny difference of the calcination condition. Simultaneously, the molecular weight of the template has a prominent effect on the surface area and total pore volume of the obtained mesoporous alumina microfibers, i.e., the mesoporous alumina microfibers prepared by using the PEG templates with little molecular weight have higher surface area and total pore volume. This may be contacted with the short chain length of the PEG with small molecular weight. Using the synthesis method in this paper, we can obtain the alumina microfibers with mesoporous structure, which have the different mesoporous parameters, through simple adjusting the molecular weight of the surfactant PEG. The above data suggest the PEG, which has been shown to be a templating to the formation of 1D nanomaterial, indeed played a role in the formation of the fiber-like alumina. However it has little contribution to the formation of the mesoporosity of the alumina microfibers. These mesopores may be formed with the amorphous alumina framework during gases burning out in the thermal calcination process [11,12].

Small-angle powder X-ray diffraction (XRD) patterns of alumina microfibers prepared by PEG templates with different molecular weight and calcined at different calcination temperatures were presented in Fig. 6. All XRD patterns exhibit one low angle peak in 2θ at around 0.9°, which signifies the presence of mesoporous structure with a pore structure lacking long range order, this is in good agreement with the TEM images of the calcined alumina microfibers. The small-angle XRD of the alumina microfibers at different calcination temperature also indicate that the mesoporosity of this alumina material can be maintained at 1373 K. The experimental results shown that the mesoporous alumina prepared in this study have high thermal stability.

In order to test the adsorption property of the as-synthesized alumina microfibers with mesoporous structure, the catalytic activity in terms of NO conversion has been studied for some as-synthesized mesoporous materials as a function of temperature. Steady-state isothermal experiments at three different temperatures (350, 400 and 450 °C) were carried out. Experimental

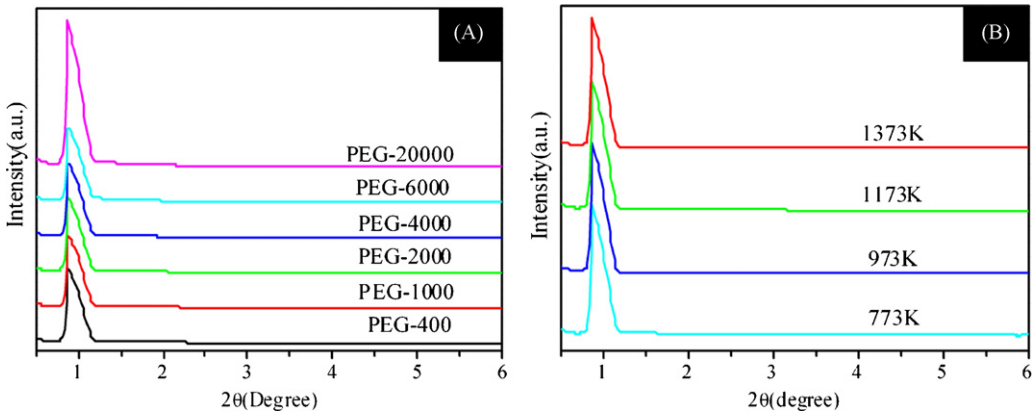

Fig. 6. Small-angle XRD patterns of as-synthesized samples calcined at 773 K (A) and PEG-20000 assisted as-synthesized sample calcined at different temperatures.

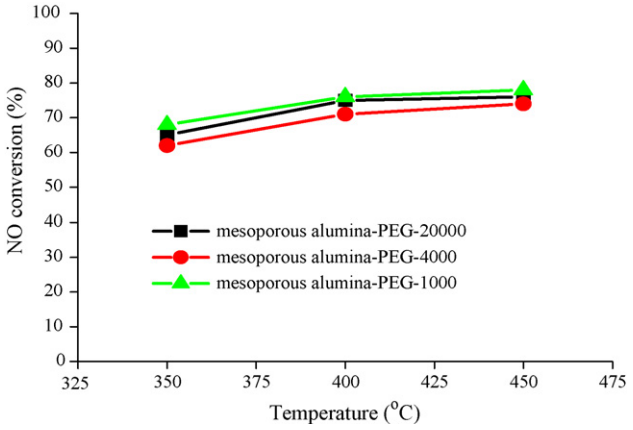

Fig. 7. Stationary conditions. NO conversion with alumina microfibers synthesized using PEG with different molecular weight. Calcination condition: 773 K, 2 h.

conditions were chosen to be close as possible to real conditions. Fig. 7 shows the NO conversion rate of the three mesoporous alumina prepared by PEG templates with different molecular weight (M_n = 1000, 4000, and 20,000) as a function of temperature. The catalystic activity of three mesoporous alumina without doped catalysts is quite similar under stationary conditions. NO conversion varies from 60% to nearly 80%, showing a dependence on temperature. As expected for a catalytic process, a higher temperature causes higher NO conversions to a certain extend. The higher NO conversion in this study is mainly caused by the high surface area of the as-synthesized alumina microfibers with mesoporous structure.

4. Conclusions

The AACH microfibers have been synthesized by a facile hydrothermal route in the presence of PEG templates with different molecular weight. By calcining the as-prepared AACH microfibers, the alumina microfibers with mesoporous structure were obtained, well inheriting the shapes of the AACH microfibers. The length and diameter of these alumina microfibers are about 10 μm and 300–500 nm, respectively. All these alumina microfibers prepared by the PEG templates with different molecular weight have the different high surface area but the nearly same pore diameter about 3.5 nm. The results indicated that the PEG template indeed played a role in the formation of the fiber-like alumina, but the mesopores within the alumina microfibers may be formed with the amorphous alumina framework during gases burning out in the thermal calcination process. Especially, the mesoporosity of these alumina microfibers can be maintained at 1373 K. This shows that the thermal stability of mesoporous alumina prepared by this method is very high. The higher adsorption property of the as-obtained mesoporous alumina is mainly due to its high surface area. Due to its unique mesoporous and high thermal stability, those as-prepared alumina microfibers may have potential applications in catalysts and catalyst supports even in high temperature.

References

[1] C.T. Lresge, M.E. Leonowiez, W.J. Roth, J.C. Beck, Nature 359 (1992) 710–712.
[2] S.A. Bagshaw, E. Prouzet, T.J. Pinnavaia, Science 269 (1995) 1442–1443.
[3] D. Zhao, Q. Huo, J. Feng, B.F. Chmelka, G.D. Stucky, J. Am. Chem. Soc. 120 (1998) 6024–6036.
[4] A. Khaleel, Microporous Mesoporous Mater. 54 (2002) 37–49.
[5] M. Trueba, S.P. Trasatti, Eur. J. Inorg. Chem. 17 (2005) 3393–3403.
[6] B. Kasprzyk-Hordern, Adv. Colloid Interface Sci. 110 (2004) 19–48.
[7] J.C. Ray, K.S. You, J.W. Ahn, W.S. Ahn, Microporous Mesoporous Mater. 100 (2007) 183–190.
[8] J.W. Park, D.S. Jung, M.E. Seo, S.Y. Kim, W.J. Moon, C.H. Shin, G. Seo, Microporous Mesoporous Mater. 112 (2008) 458–466.
[9] M. Yada, H. Hiyoshi, K. Ohe, M. Machida, T. Kijima, Inorg. Chem. 36 (1997) 5565–5569.
[10] K. Niesz, P. Yang, G.A. Somorjai, Chem. Commun. 15 (2005) 1986–1988.
[11] C.C. Yu, L.X. Zhang, J.L. Shi, J.J. Zhao, J.H. Gao, D.S. Yan, Adv. Funct. Mater. 18 (2008) 1544–1554.
[12] C.C. Yu, X.P. Dong, L.M. Guo, J.T. Li, F. Qin, L.X. Zhang, J.L. Shi, D.S. Yan, J. Phys. Chem. C 112 (2008) 13378–13382.
[13] Y. Kim, C. Kim, I. Choi, S. Rengaraj, J. Yi, Environ. Sci. Technol. 38 (2004) 924–931.
[14] T. Oikawa, T. Ookoshi, T. Tanaka, T. Yamamoto, M. Onaka, Microporous Mesoporous Mater. 74 (2004) 93–103.
[15] M.H. Cao, Y.H. Wang, C.X. Guo, J. Nanosci. Naonotechnol. 4 (2004) 824–828.
[16] Z.Q. Li, Y.J. Xiong, Y. Xie, Inorg. Chem. 42 (2003) 8105–8109.
[17] P.T. Hammond, Adv. Mater. 16 (2004) 1271–1293.
[18] S. Music, D. Dragcevic, S. Popovic, Mater. Lett. 40 (1999) 269–274.
[19] A. Boyano, M.J. Lazaro, C. Cristiani, F.J. Maldonado-Hodar, P. Forzatti, R. Moliner, Chem. Eng. J. 149 (2009) 173–182.
[20] S. Kato, T. Iga, S. Hatano, M. Minowa, Y. Isawa, U.S. Patent 4,053,579 (1975).
[21] C. Ma, X. Zhou, X. Xu, T. Zhu, Mater. Chem. Phys. 72 (2001) 374–379.
[22] X. Sun, J. Li, F. Zhang, X. Qin, Z. Xiu, H. Ru, J. Am. Ceram. Soc. 86 (2003) 1321–1325.
[23] Z. Li, X. Feng, H. Yao, X. Guo, J. Mater. Sci. 39 (2004) 2267–2269.
[24] K. Morinaga, T. Torikai, K. Nakagawa, S. Fujino, Acta Mater. 48 (2000) 4735–4741.
[25] P. Bai, F.B. Su, P.P. Wu, L.K. Wang, F.Y. Lee, L. Lv, Z.F. Yan, X.S. Zhao, Langmuir 23 (2007) 4599–4605.
[26] C.C. Ma, X.X. Zhou, X. Xu, T. Zhu, Mater. Chem. Phys. 72 (2001) 374–379.
[27] O. Yong-Taeg, S.W. Kim, D.C. Shin, Colloids Surf. A: Physicochem. Eng. Aspects 313–314 (2008) 415–418.